THE JOURNAL OF PHYSICAL CHEMISTRY C

Article

pubs.acs.org/JPCC

Surface Plasmon Resonance Determination of the Binding Mechanisms of L-Cysteine and Mercaptoundecanoic Acid on Gold

Nancy Tawil,[†,‡,∥] Ali Hatef,[†] Edward Sacher,*[,‡] Mathieu Maisonneuve,[†] Thomas Gervais,[§] Rosemonde Mandeville,[∥] and Michel Meunier[†,‡]

[†]Laser Processing and Plasmonics Laboratory, Department of Engineering Physics, [‡]Laboratory for the Analysis of the Surfaces of Materials, Department of Engineering Physics, and [§]Department of Engineering Physics, École Polytechnique de Montréal, Case Postale 6079, succursale Centre-Ville, Montréal, Québec, H3C 3A7 Canada

[∥]Biophage Pharma, 6100 Royalmount, Montreal, QC H4P 2R2, Canada

ABSTRACT: Surface plasmon resonance was used for the real-time monitoring of the formation of self-assembled monolayers of L-cysteine and 11-mercaptoundecanoic acid (MUA) on gold surfaces. We provide comparative details on the kinetics of the assembly of short thiols with multiple functional groups, as opposed to longer alkanethiols with fewer functional groups. Our results indicate that the adsorption of L-cysteine is a rapid process, involving both amino- and thiol-Au interactions, followed by the exchange of amino-Au to thiol-Au species and the physisorption of a second cysteine layer. The formation of MUA is also rapid, followed by a slower structural rearrangement of the monolayer. We find that monolayer formation, for both L-cysteine and MUA, is described by the Langmuir isotherm at low concentrations only. Numerical models are introduced to describe the assembly of both higher and lower concentrations of thiolated molecules on gold.

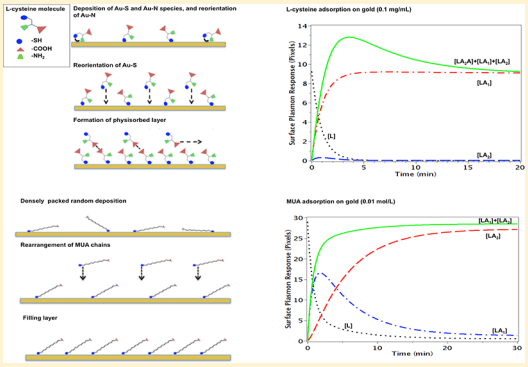

INTRODUCTION

The attachment of molecules to a support, resulting in their immobilization, has found multiple applications in industrial chemistry and biosensing devices. Self-assembled monolayers (SAMs), composed of chemisorbed species, play a fundamental role in altering the interfacial properties of metals, polymers, and semiconductors. Notably, the affinity of thiols for gold permits the generation of well-defined surfaces with various desirable chemical functionalities and optical properties. Currently, thiols are the most utilized form of organic thin-film material.

The physical and structural characterizations of SAMs have been extensively reviewed in the literature.[1,2] However, despite considerable efforts to study their formation on gold, little is known about their real-time adsorption kinetics.[3] Although the chemistry appears to be straightforward, the details of the assembly at the interface are still approximated qualitatively by a Langmuir absorption model.[4] Originally, SAM formation was thought to occur by the activation of the S−H bond at the surface.[1] Alternative interpretations, such as a two-stage adsorption process for longer chains, have been reported, where the surface coverage reaches 60−90% of its maximum in the first few minutes, followed by a slower period of several hours, before which maximum coverage is attained.[5,6] Some authors have shown that the dynamics of this adsorption follows a simple Langmuir rate model,[7] whereas others have shown that a diffusion-controlled Langmuir model is a better fit at low concentrations.[8] Such contradictory results could, in part, be attributed to one or more of several sources, such as the presence of contaminants on the gold surface, the effects of the concentrations of solvent and thiol, and the sensitivity of the method used.[7] Previous studies, using atomic force microscopy,[9] ellipsometry,[10,11] and contact angle measurements,[12] were limited in time resolution, which is why we chose to use surface plasmon resonance (SPR), making real-time adsorption analysis possible. This article describes the real-time formation of SAMs of L-cysteine and 11-mercaptoundecanoic acid (MUA) at different concentrations on a gold sensor platform using SPR and evaluation by numerical methods. Our purpose, in carrying out these measurements with both L-cysteine and MUA, was to compare the binding characteristics of both molecules and establish each molecule's validity and applicability as a linker element for use in biosensing.

EXPERIMENTAL SECTION

Preparation of Au Surfaces. Biacore Platypus biosensor chips, to be described below, were used as the gold surface. Prior to modification, they were placed in freshly prepared "Piranha" solution, a 7:3 mixture of concentrated H_2SO_4 and 30% H_2O_2 (Caution: piranha solution reacts vigorously with organics and can splatter), at room temperature for 30 min, then rinsed thoroughly with Milli-Q water (Millipore,

Received: January 25, 2013
Revised: March 13, 2013
Published: March 14, 2013

   dx.doi.org/10.1021/jp400873t | J. Phys. Chem. C 2013, 117, 6712−6718

Mississauga, Ont.), ultrasonicated in water for 15 min, and dried in a nitrogen flow.

Chemicals. L-Cysteine, MUA, sodium chloride, magnesium sulfate, and phosphate-buffered saline (PBS) were purchased from Sigma-Aldrich.

Surface Plasmon Resonance Apparatus. Superluminescent light-emitting diode (SLED), emitting at 650 nm, was used as the light source. An achromatic lens produced a collimated beam, which passed through a polarizer. The linearly *p*-polarized light was focused by a lens and then used to excite surface plasmons on the sensing surface, situated on top of a coupling prism. A commercial sensing surface (Platypus Technologies), consisting of a glass microscope slide (BK7) covered by an adhesion layer of 5 nm of titanium and a sensing layer of 50 nm of gold, was placed in an oil-immersion contact (Cargille Laboratories) on the top of the coupling prism. For the real-time tests, a flow injection double-channel-measuring cell, with a 12 μL volume, was developed. The entire system was placed on a goniometer stage, with 2-D linear translation for exact beam angle and position, permitting surface plasmon excitation at the gold/adjacent medium interface. The spatial distribution of the reflected light intensity was recorded by a CCD camera (Hamamatsu C4742-95) and examined by an appropriate software image treatment. A more detailed description of the system can be found in ref 13.

SPR Detection L-Cysteine and MUA Adsorption to Gold. The cleaned gold slides were placed on the SPR coupling prism, using a refractive index-matching immersion liquid (Cargille Laboratories). Prior to L-cysteine injection, Milli-Q water was injected at a flow rate of 111 μL/min, controlled by a peristaltic pump, to obtain a baseline. Solutions of different concentrations of L-cysteine in Milli-Q water were subsequently pumped into the SPR apparatus at the same flow rate. This was followed by a washing step with Milli-Q water.

In the case of water-insoluble MUA, ethanol was first injected onto the chip, followed by injection of different concentrations of freshly prepared solutions of MUA in ethanol, and ethanol was used for the washing step.

RESULTS AND DISCUSSION

L-Cysteine. Planar gold was used to characterize the attachment of L-cysteine and MUA because of the ease of preparation of such substrates and their compatibility with SPR spectroscopy.

L-Cysteine is a neutral amino acid with hydrophilic properties. It is reported to bind to gold via its thiol group. However, it has two other terminal groups that are chemically active, $-NH_2$ and $-COOH$, which, depending on the pH, may play a role in the formation and organization of the monolayer.

The Langmuir adsorption isotherm is based on the fraction of available sites that have already reacted. Thus, the rate of adsorption is expected to follow Langmuir adsorption kinetics

$$\frac{d\Theta}{dt} = k_a(1 - \Theta)c - k_d\Theta \quad (1)$$

where Θ is the fraction of the gold surface that is covered, $(1 - \Theta)$ is the uncovered fraction, k_a is the association constant, k_d is the dissociation constant, and c is the concentration of the thiol solution.

We have examined L-cysteine adsorption kinetics at several concentrations. The raw data are a direct result of the refractive index change induced by L-cysteine adsorption onto the gold surface.

Figure 1 provides insight into the relationship among physisorption, chemisorption, concentration, and time. In this

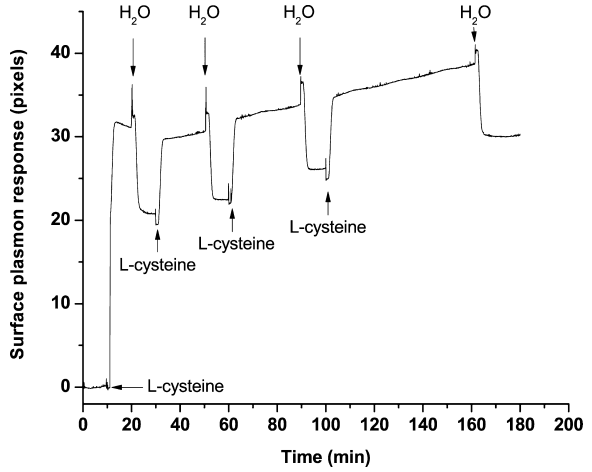

Figure 1. Relationship between physisorption and chemisorption of L-cysteine on gold. A baseline was created by flowing Milli-Q water for 10 min over the sensor surface. Following this, a solution of 1 mg of L-cysteine per milliliter of Milli-Q water was injected for varying periods of time (10, 20, 30, and 60 min), each followed by a washing step of 10 min duration. The first 30 min shows a negative slope, whereas there is a positive shift of the plasmon response within 30 min after the initial injection of L-cysteine. The physisorption and chemisorption components responsible for the plasmon shift reach equilibrium 30 min after L-cysteine injection.

experiment, Milli-Q water was first injected for 10 min to create a baseline, after which 1 mg/mL of L-cysteine was injected for a period of 10 min, followed by a 10 min washing step. The same solution of L-cysteine was further injected for longer periods of time (20, 30, and 60 min), each separated by a washing step of 10 min to remove the loosely bound, physisorbed L-cysteine molecules. Our results show that the slope is negative for the first 30 min but goes from negative to positive over a longer time period (between 30 and 180 min). The equilibrium between chemisorption (SPR signal following washing) and physisorption (SPR signal after further injection of 1 mg/mL of L-cysteine) is attained in <30 min after initial injection, as is shown by the identical slopes of both signals. Moreover, it can be seen that the rearrangement of the adsorbed thiol is a very slow process, taking hours. Because the strength of the -SH chemisorption bond is large (125−167 kJ/mol),[14,15] any desorption of the adsorbed thiol is assumed to be negligible. This leads us to believe that the loss of plasmon response units, on washing, is due to the removal of a second, loosely bound layer. This is corroborated by other studies, showing the prevalence of a double-layer configuration of L-cysteine.[16] Moreover, in an XPS study on self-assembled films, Cavaleleri et al. reported that for L-cysteine a physisorbed layer forms on top of the chemisorbed monolayer and that the analysis of the N1s spectrum indicated the prevalence of a zwitterionic state.[17] It has also been reported that molecules tend to adopt conformations that allow high degrees of van der Waals interactions and hydrogen bonding to minimize the free energy of the organic layer.[18,19] The washing away of physisorbed L-cysteine molecules, electrostatically attached to the chemisorbed monolayer, appears to explain the loss of surface plasmon response after the washing step. This is supported by Abraham et al., where solid-state NMR spectroscopy showed

dx.doi.org/10.1021/jp400873t | J. Phys. Chem. C 2013, 117, 6712−6718

that cysteine adsorbs to gold via the formation of a two-layer boundary, in which a second layer of L-cysteine molecules interacts with the cysteine molecules chemisorbed on gold through hydrogen bonding between the charged groups of the zwitterions.[20]

Moreover, because physi- and chemisorption quickly reach equilibrium, we conclude that reaching a steady-state condition is a consequence of the ordering and rearrangement of the monolayer chains alone.

Figure 2 shows the real-time adsorption of several concentrations of L-cysteine on gold at 295 K. Lower

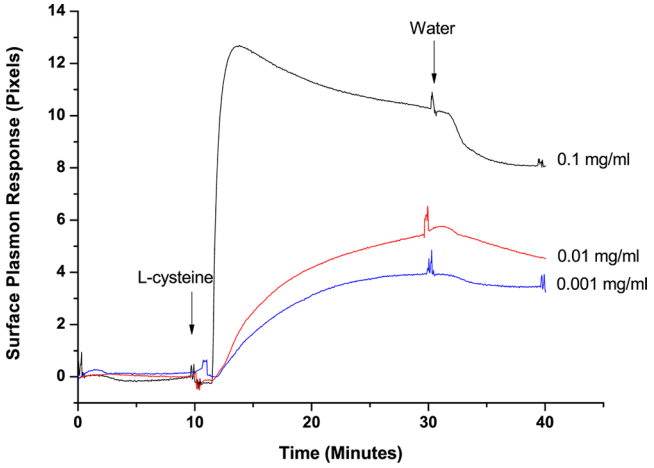

Figure 2. SPR sensogram of the adsorption of different concentrations of L-cysteine on gold. A baseline was created by injecting Milli-Q water on the sensor surface for a period of 10 min. This was followed by the injection of different concentrations of L-cysteine (0.001, 0.01, and 0.1 mg/mL). Subsequently, a washing step was performed, in which Milli-Q water was injected on the sensor surface for another 10 min.

concentrations of L-cysteine (0.001 and 0.01 mg/mL) appear to follow simple Langmuir adsorption kinetics whereas the higher concentration (0.1 mg/mL) does not. From the SPR data for lower concentrations, we determine the kinetic parameters using eq 1, k_a = 3.87 L mol^{-1} s^{-1} and k_d = 0.00266 s^{-1}, making K_{eq} = 1.455 × 10^3 L mol^{-1} and ΔG_{ads} = 17.9 kJ mol^{-1}. Thus, desorption does not play an important role in the formation of the chemisorbed layer and that most of the adsorption sites on the surface are occupied. Because mass transfer is central to exploring biochemical reactions in a surface-based detection system, we wish to ensure that the SPR signal is indeed reaction-limited; that is, the diffusion time of the analyte to the surface is much smaller than the binding time. To verify this property, we use the expressions for the convective/diffusive length, $\zeta = LWD/Qh$, and the Damköler number, $Da = k_aC_{s0}d(h)/D$, for a first-order surface reaction; L is the length of the reactive zone, W is the channel width, D is the diffusivity of the analyte, Q is the flow rate, and $d(h) = h^*\zeta^{1/3}$ is the characteristic thickness of the diffusive boundary layer as a function of channel height. C_{s0}, the initial surface concentration of binding sites, was found to be typical of a densely packed thiol monolayer (~7.47 × 10^{-6} mol/m^2).[19] We find that for both L-cysteine and MUA $\zeta \ll 1$ (~10^{-5}), suggesting that mass transfer occurs through a thin boundary layer of characteristic thickness $d \approx 1$ μm, greatly speeding up diffusion. Furthermore, the Damköler number is on the order of 10^{-3}, indicating that the transport is limited by the process on the surface and that a constant concentration profile can be expected across the channel.[21] Therefore, the diffusive effects are negligible.

Figure 3 models the adsorption of L-cysteine on gold. The rapid response in the first few minutes is attributed to the chemisorption of the L-cysteine via both amine and thiol groups. The subsequent negative slope is attributed to the reorientation of that fraction of the L-cysteine, initially adsorbed via its amine end, to a more stable Au−S bound species. This is in agreement with Kuhnle et al.,[22] where L-cysteine is shown to be bound by both sulfur−gold and amino−gold bonds. L-Cysteine molecules can exist in either neutral or zwitterionic forms, depending on the pH of the solution. It is believed that at low coverage, the neutral form of L-cysteine is present simultaneously with zwitterionic form, whereas the zwitterionic form is dominant at monolayer coverage and beyond.[17,23,24] Furthermore, because the L-cysteine solution has a pH of 4.7, its amine is protonated (NH_3^+),[25] enabling an additional layer,[26] physisorbed by electrostatic interactions to the chemisorbed layer. We present a simulation in Figure 3b,c that qualitatively shows the interaction. The binding kinetics of a surface-immobilized ligand to capture an analyte in solution, including the second-layer formation, is modeled as a four-step reaction. For L-cysteine, the net reaction rates of the different concentrations follow Langmuir adsorption kinetics, as indicated by the set of equations:

$$\frac{d[L]}{d\tau} = -K_{a1}[A][L] - K_{a2}[A][L] + K_{d1}[LA_1] + K_{d2}[LA_2] + \Phi K_r[LA_2] \quad (2\text{-a})$$

$$\frac{d[LA_1]}{d\tau} = K_{a1}[A][L] - K_{d1}[LA_1] + (1-\Phi)K_r[LA_2] \quad (2\text{-b})$$

$$\frac{d[LA_2]}{d\tau} = K_{a2}[A][L] - K_{d2}[LA_2] - K_r[LA_2] \quad (2\text{-c})$$

$$\frac{d[LA_2A]}{d\tau} = K_{a3}[A][LA_2] - K_{d3}[LA_2A] \quad (2\text{-d})$$

For simplicity, we have normalized all terms by a constant, having units of min^{-1}; that is, $\tau = K_0t$. [L] and [A] represent, respectively, the concentrations of surface ligands and analytes in bulk solution. [LA_1], [LA_2], and [LA_2A] represent, respectively, the surface densities of adsorbed analyte molecules via thiol group, amine group, and second-layer. [A] is assumed to be constant with time, whereas [L] is depleted due to the binding reaction. Φ is the unreacted fraction of the gold surface after the reorientation of L-cysteine molecules, $(1 - \Phi)$ is the reacted fraction, K_{ai} (i = 1, 2, 3) is the normalized association constant, K_{di} (i = 1, 2, 3) is the normalized dissociation constant, and K_r is the normalized reorientation constant. The initial conditions at time t = 0 are [L] = 10 and [LA_1] = [LA_2] = [LA_2A] = 0. In these equations, the positive and negative terms show the formation and breaking, respectively, of the ligands and complexes in the system. For example, in eq 2-a, the first and second terms represent the breaking of the ligands for a constants value of analyte concentration, which leads to the formation of the [LA_1] and [LA_2] complexes. The third and the fourth terms represent the formation of ligands by dissociation of the [LA_1] and [LA_2] complexes. Finally, the fifth term represents the formation of ligand by reorientation of the [LA_2] complex. We used a numerical solver, available in the

dx.doi.org/10.1021/jp400873t | J. Phys. Chem. C 2013, 117, 6712−6718

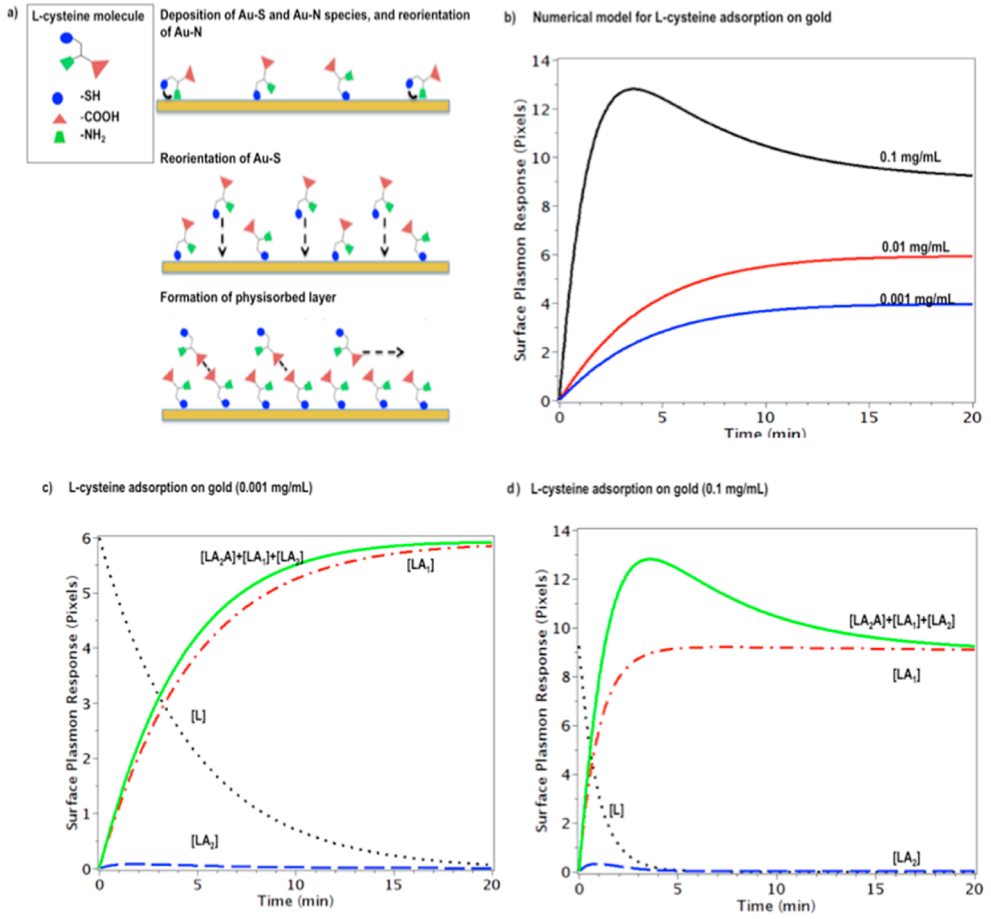

Figure 3. Adsorption kinetics of L-cysteine on gold. (a) L-Cysteine may attach to gold via its thiol or amine groups. The amine−gold interaction is short-lived, and the L-cysteine reorients to attach via its thiol group. This is followed by an ordering of the chemisorbed layer and the subsequent formation of a second, physisorbed, layer atop the chemisorbed L-cysteine species. (b) Numerical model for different concentrations of L-cysteine. (c) Surface plasmon resonance of 0.001 mg L-cysteine/mL H_2O profile versus time. The dotted, dash-dotted, dashed, and solid curves represent [L], [LA_1], [LA_2], and [LA_2A]+[LA_1]+[LA_2], respectively. (d) Surface plasmon resonance of the 0.1 mg L-cysteine/mL H_2O profile versus time. The dotted, dashed-dotted, dashed, and solid curves represent [L], [LA_1], [LA_2], and [LA_2A]+[LA_1]+[LA_2], respectively.

Maple software package (Maplesoft, a division of Waterloo Maple, 2012) to solve the coupled differential equation system.

The model applies at both lower (Figure 3c) and higher concentrations (Figure 3d). It can be seen that our model can be simplified to the Langmuir model at low concentrations (Figure 3b). In the Langmuir model, θ represents the surface occupied by the analyte, which is equivalent to [LA] in the previously described model, and the unbound surface $(1-\theta)$ is equivalent to (L). Thus, although all terms in the model are necessary at higher concentrations, reactions with lower adsorption rates (i.e., [LA_2]), become negligible at lower concentrations, and the model is simplified to the Langmuir isotherm, using eq 2-b. This is also observed experimentally.

11-MUA. The common protocol for the generation of alkanethiol SAMs involves the immersion of cleaned substrates in dilute ethanolic solutions of thiols for several hours at room temperature. Ethanol is used because alkanethiols, such as MUA, are not soluble in water. Although the dielectric constant of ethanol (24.3) is lower than that of water (78.5), it is still much higher than that of nonpolar solvents (e.g., ϵ_{hexane} = 1.9).[27] Figure 4 follows the real-time attachment of MUA to a gold surface. Ethanol was first injected for 10 min to create a baseline, following which several concentrations (10^{-4}, 10^{-3}, and 10^{-2} mol L^{-1}) of MUA in ethanol were injected for 20 min.

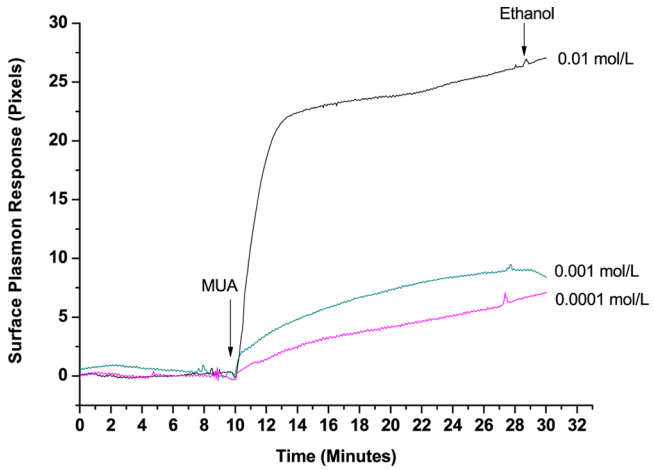

Figure 4. Various concentrations of MUA adsorbed onto gold. An ethanol baseline was first obtained; after 10 min, a solution of MUA was injected for another 20 min, followed by a short ethanol washing step.

Finally, ethanol was reinjected for the washing step. Exposure of the gold surface to MUA resulted in a rapid increase in the

dx.doi.org/10.1021/jp400873t | J. Phys. Chem. C 2013, 117, 6712−6718

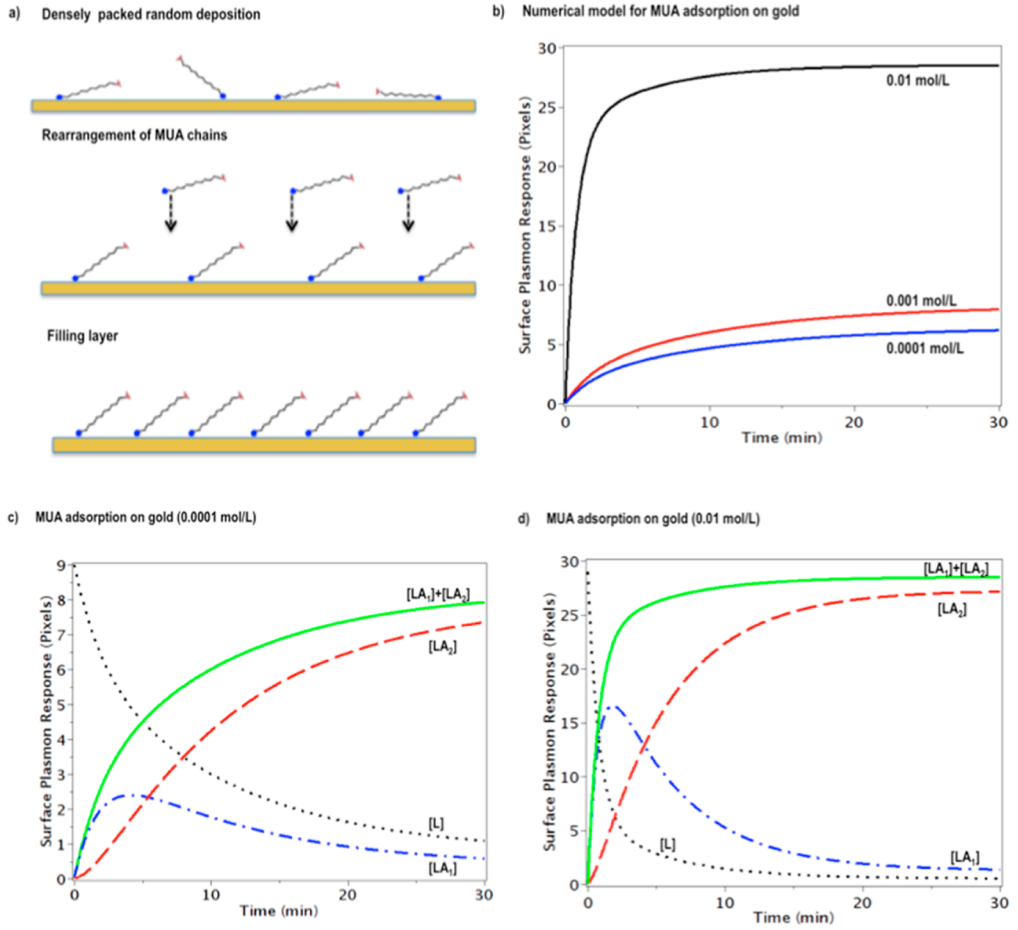

Figure 5. Model for the attachment of MUA on gold. (a) MUA chains first deposit on the surface of the gold in a random manner, followed by their rearrangement, which provides more sites for further chain attachment to gold. (b) Numerical model for different concentrations of L-cysteine. (c) Surface plasmon resonance profile of 0.01 mol MUA/L of ethanol versus time. The dotted, dash-dotted, dashed, and solid curves represent [L], [LA_1], [LA_2], and [LA_1]+[LA_2], respectively. (d) Surface plasmon resonance profile of 0.001 mol MUA/L of ethanol versus time. As in panel b, the dotted, dash-dotted, dashed, and solid curves represent [L], [LA_1], [LA_2], and [LA_1]+[LA_2], respectively.

SPR response in the first 30 min, followed by a slow increase over the next 2 h (data not shown).

A rapid coverage of the gold is achieved within the first few minutes, followed by a slower increase in the SPR response. The attachment of MUA to the gold surface also follows a two-step process but is different from that of L-cysteine (Figure 5a). We hypothesize that the chains deposit in a random manner, followed by their restructuring into a SAM. The gradual increase in plasmon response, over the next few hours, indicates that as expected sites on the gold surface slowly become available because this reorientation makes new sites available, permitting further adsorption. Differences in models for low and high concentrations are attributed to a loose, horizontal configuration for low-coverage adsorption, whereas a compact, vertical phase is observed for higher coverage.[28] Our results are in agreement with recent studies, showing that solutions with lower concentrations of SAMs do not have the same physical properties as those created from more concentrated solutions.[29] From lower concentrations of MUA, we determine k_a = 1.233 L mol^{-1} s^{-1} and $k_d = 8.86 \times 10^{-4}$ s^{-1}. A value of ΔG_{ads}= −17.8 kJ mol^{-1} was obtained, which is similar to the value estimated in the literature.[30,31]The low value of k_d tells us that desorption does not play an important role in the formation of the monolayer.

For MUA, the net reaction rates of the different concentrations are written as:

$$\frac{d[L]}{d\tau} = -K_{a1}[A][L] - K_{a2}[A]\Phi[L] + K_{d1}[LA_1] + K_{d2}[LA_2] + \Phi K_r[LA_1] \quad (3\text{-a})$$

$$\frac{d[LA_1]}{d\tau} = K_{a1}[A][L] - K_{d1}[LA_1] - K_r[LA_1] \quad (3\text{-b})$$

$$\frac{d[LA_2]}{d\tau} = K_{a2}[A]\Phi[L] - K_{d2}[LA_2] + (1-\Phi)K_r[LA_1] \quad (3\text{-c})$$

In eqs 3-a to 3-c, [LA_1] and [LA_2] represent the surface densities of MUA chains on the surface of the gold in a random (dense random deposition) and aligned manner (filling layer), respectively (Figure 5a). This is in agreement with multiple studies reporting an intermediate low-coverage phase arising prior to the nucleation and growth of the upright higher coverage phase.[32] Using these equations, we numerically modeled the adsorption of MUA on gold (Figure 5b). In this process, MUA first deposits on gold in a random fashion ([LA_1]), it then reorients with a rate of K_r, providing more space (Φ [L]) for further MUA attachment to gold ([LA_2]). As with L-cysteine, the model applies to both lower (Figure 5c)

dx.doi.org/10.1021/jp400873t | J. Phys. Chem. C 2013, 117, 6712−6718

and higher concentrations (Figure 5d) of MUA. The initial conditions for 0.01 mol/L at time $t = 0$ are $[L] = 29$ and $[LA_1] = [LA_2] = 0$.

Comparison of Kinetic Profiles of L-Cysteine and MUA. Although there is an extensive literature on alkanethiol SAMs, those of amino acids, such as L-cysteine, have been overlooked in comparison. In the case of L-cysteine, the presence of both the carboxy and the amino groups confers broader possibilities for metal−molecule and molecule−molecule interactions through electrostatic, hydrogen, and peptide bonding. Understanding the differences in the adlayer structure of L-cysteine and MUA on gold surfaces is an important issue for biosensing purposes. L-Cysteine is a much smaller molecule and its zwitterionic state results in various intermolecular forces that govern its interaction with the metal surface. Thus, even though it is believed that the chemical reaction that binds cysteine to gold is similar to that that permits the formation of MUA SAMs, we have found that the thiol and amino groups of L-cysteine first compete for the adsorption on the metal. Our results are in agreement with those of various groups whose findings show that cysteine most likely employs multiple functional groups in its bonding to gold surfaces.[22,28] Over a period of time, the thermodynamically more stable SH groups replace NH groups on gold, giving additional space on the surface, resulting in increased bonding and, ultimately, packing the surface. This primary rearrangement of the groups is not seen with MUA because the primary covalent interaction is due to the thiol group. That group is thus more readily attached in the case of MUA, explaining why very little desorption is seen when washing the surface compared with L-cysteine. Moreover, L-cysteine is found in a zwitterionic form, and electrostatic interactions expose the amine group, permitting possible molecular coordination. Furthermore, the zwitterionic form facilitates the coupling of unbound molecules, provoking the formation of a second, physisorbed, layer, a phenomenon not seen with MUA. We believe that the zwitterionic character of cysteine is directly linked to its ability to form H-bonded molecular networks. This hydrogen-bonded network will affect the conformation and the overall packing of the SAM.[18] Moreover, the geometrical structure of the H-bonded network was found to be dependent on both layer coverage and temperature.[33] To that effect, Renzi et al. found that, at room temperature, L-cysteine first-layer deposition was quite heterogeneous and that both weakly and strongly bound molecules coexist. This could partially explain the negative slope observed in the first adsorption cycle of L-cysteine. Finally, MUA SAMs were found to be more stable than those of L-cysteine because long-chain adsorbates are more robust than their shorter counterparts due to contributions of attractive lateral interactions.[2] It should be noted that studies on the molecular diffusion mechanisms of cysteine on gold show that the substrate is central to the formation of the monolayers, a factor not accounted for in the model described.[34] New structures not previously reported, such as cysteine trimers, molecular rows, or ordered networks, can form due to surface defects. In the case of L-cysteine, it has been postulated that the amount of zwitterionic fraction, when compared with the acidic fraction, is dependent on the lattice symmetry of the metal surface.[24] Gonella et al. believe that the neutral acidic fraction, relevant only at low coverage, is likely related to isolated molecules or to the formation of dimers and is possibly related to the surface morphology of the substrate. Additional studies clarifying the substrate impact on SAM formation are desirable.

CONCLUSIONS

The adsorption characteristics of thiol-containing molecules are necessary for applications involving the attachment of recognition elements to a functionalized surface. We have considered their attachment to gold surfaces for plasmon resonance biosensing applications. We have shown that the self-assembly of L-cysteine differs from that of MUA. It is evident that the deposition process involves not only contributions of the sulfur bonds but also those of other existent functional groups as well as those of subsequent noncovalent adsorbed molecules. Both the amine and thiol groups of L-cysteine contribute to its initial attachment, followed by replacement of the amine-gold complex initially formed with the more stable thiol-gold complex. The reorganization of L-cysteine creates more space on the gold surface, and the zwitterionic form of the molecule permits the physisorption of a second layer through electrostatic interactions. Such a structure has high potential for further biofunctionalization. MUA deposits randomly onto the surface of gold as a SAM and slowly reorganizes into a denser, vertical state.

AUTHOR INFORMATION

Notes

The authors declare no competing financial interest.

ACKNOWLEDGMENTS

We thank NanoQuébec for its financial support and Dr. Paul. Boyer and Etienne Boulais for their insight and assistance.

REFERENCES

(1) Dubois, L. H.; Nuzzo, R. G. Synthesis, Structure, And Properties of Model Organic-Surfaces. *Annu. Rev. Phys. Chem.* **1992**, *43*, 437−463.
(2) Schreiber, F. Structure and Growth of Self-Assembling Monolayers. *Prog. Surf. Sci.* **2000**, *65*, 151−256.
(3) Bieri, M.; Burgi, T. Adsorption Kinetics, Orientation, and Self-Assembling of *N*-Acetyl-L-cysteine on Gold: A Combined ATR-IR, PM-IRRAS, and QCM Study. *J. Phys. Chem. B* **2005**, *109*, 22476−22485.
(4) Tielens, F.; Santos, E.; AuS; Bond, S. H. Formation/Breaking during the Formation of Alkanethiol SAMs on Au(111): A Theoretical Study. *J. Phys. Chem. C* **2010**, *114*, 9444−9452.
(5) Hu, K.; Bard, A. J. In Situ Monitoring of Kinetics of Charged Thiol Adsorption on Gold Using an Atomic Force Microscope. *Langmuir* **1998**, *14*, 4790−4794.
(6) DeBono, R. F.; Loucks, G. D.; DellaManna, D.; Krull, U. J. Self-Assembly of Short and Long-Chain *n*-Alkyl Thiols onto Gold Surfaces: A Real-Time Study Using Surface Plasmon Resonance Techniques. *Can. J. Chem.* **1996**, *74*, 677−688.
(7) Pan, W.; Durning, C. J.; Turro, N. J. Kinetics of Alkanethiol Adsorption on Gold. *Langmuir* **1996**, *12*, 4469−4473.
(8) Subramanian, R.; Lakshminarayanan, V. A Study of Kinetics of Adsorption of Alkanethiols on Gold Using Electrochemical Impedance Spectroscopy. *Electrochim. Acta* **2000**, *45*, 4501−4509.
(9) Alves, C. A.; Smith, E. L.; Porter, M. D. Atomic Scale Imaging of Alkanethiolate Monolayers at Gold Surfaces with Atomic Force Microscopy. *J. Am. Chem. Soc.* **1992**, *114*, 1222−1227.
(10) Prato, M.; Alloisio, M.; Jadhav, S. A.; Chincarini, A.; Svaldo-Lanero, T.; Bisio, F.; Cavalleri, O.; Canepa, M. Optical Properties of Disulfide-Functionalized Diacetylene Self-Assembled Monolayers on Gold: A Spectroscopic Ellipsometry Study. *J. Phys. Chem. C* **2009**, *113*, 20683−20688.

(11) Prato, M.; Moroni, R.; Bisio, F.; Rolandi, R.; Mattera, L.; Cavalleri, O.; Canepa, M. Optical Characterization of Thiolate Self-Assembled Monolayers on Au(111). *J. Phys. Chem. C* **2008**, *112*, 3899−3906.
(12) Baralia, G. G.; Duwez, A. S.; Nysten, B.; Jonas, A. M. Kinetics of Exchange of Alkanethiol Monolayers Self-Assembled on Polycrystalline Gold. *Langmuir* **2005**, *21*, 6825−6829.
(13) Tawil, N.; Sacher, E.; Mandeville, R.; Meunier, M. Surface Plasmon Resonance Detection of E. coli and Methicillin-Resistant S. Aureus Using Bacteriophages. *Biosens. Bioelectron.* **2012**, *37*, 24−9.
(14) Pensa, E.; Carro, P.; Rubert, A. A.; Benitez, G.; Vericat, C.; Salvarezza, R. C. Thiol with an Unusual Adsorption-Desorption Behavior: 6-Mercaptopurine on Au(111). *Langmuir* **2010**, *26*, 17068−17074.
(15) Vericat, C.; Vela, M. E.; Benitez, G.; Carro, P.; Salvarezza, R. C. Self-Assembled Monolayers of Thiols and Dithiols on Gold: New Challenges for a Well-Known System. *Chem. Soc. Rev.* **2010**, *39*, 1805−1834.
(16) Carr, J. A.; Wang, H.; Abraham, A.; Gullion, T.; Lewis, J. P. L-Cysteine Interaction with Au-55 Nanoparticle. *J. Phys. Chem. C* **2012**, *116*, 25816−25823.
(17) Cavalleri, O.; Oliveri, L.; Dacca, A.; Parodi, R.; Rolandi, R. XPS Measurements on L-Cysteine and 1-Octadecanethiol Self-Assembled Films: A Comparative Study. *Appl. Surf. Sci.* **2001**, *175*, 357−362.
(18) Valiokas, R.; Ostblom, M.; Svedhem, S.; Svensson, S. C. T.; Liedberg, B. Thermal Stability of Self-Assembled Monolayers: Influence of Lateral Hydrogen Bonding. *J. Phys. Chem. B* **2002**, *106*, 10401−10409.
(19) Love, J. C.; Estroff, L. A.; Kriebel, J. K.; Nuzzo, R. G.; Whitesides, G. M. Self-Assembled Monolayers of Thiolates on Metals As a Form of Nanotechnology. *Chem. Rev.* **2005**, *105*, 1103−1169.
(20) Abraham, A.; Mihaliuk, E.; Kumar, B.; Legleiter, J.; Gullion, T. Solid-State NMR Study of Cysteine on Gold Nanoparticles. *J. Phys. Chem. C* **2010**, *114*, 18109−18114.
(21) Gervais, T.; Jensen, K.F. Mass Transport and Surface Reactions in Microfluidic Systems. *Chem. Eng. Sci.* **2006**, *61*, 1102−1121.
(22) Kuhnle, A.; Linderoth, T. R.; Hammer, B.; Besenbacher, F. Chiral Recognition in Dimerization of Adsorbed Cysteine Observed by Scanning Tunnelling Microscopy. *Nature* **2002**, *415*, 891−893.
(23) Cavalleri, O.; Gonella, G.; Terreni, S.; Vignolo, M.; Floreano, L.; Morgante, A.; Canepa, M.; Rolandi, R. High Resolution X-ray Photoelectron Spectroscopy of L-Cysteine Self-Assembled Films. *Phys. Chem. Chem. Phys.* **2004**, *6*, 4042−4046.
(24) Gonella, G.; Terreni, S.; Cvetko, D.; Cossaro, A.; Mattera, L.; Cavalleri, O.; Rolandi, R.; Morgante, A.; Floreano, L.; Canepa, M. Ultrahigh Vacuum Deposition of L-Cysteine on Au(110) Studied by High-Resolution X-ray Photoemission: From Early Stages of Adsorption to Molecular Organization. *J. Phys. Chem. B* **2005**, *109*, 18003−18009.
(25) Ihs, A.; Liedberg, B. Chemisorption of L-Cysteine and 3-Mercaptopropionic Acid on Gold and Copper Surfaces - an Infrared Reflection Absorption Study. *J. Colloid Interface Sci.* **1991**, *144*, 282−292.
(26) Uvdal, K.; Bodo, P.; Liedberg, B. L-Cysteine Adsorbed on Gold and Copper - an X-Ray Photoelectron-Spectroscopy Study. *J. Colloid Interface Sci.* **1992**, *149*, 162−173.
(27) Voet, D.; Voet, J. G. Biochemistry. In *Biochemistry*, 3rd ed.; John Wiley & Sons: Hoboken, NJ, 2004; Vol. *1*, p 1178.
(28) Hakkinen, H. The Gold-Sulfur Interface at the Nanoscale. *Nat. Chem.* **2012**, *4*, 443−455.
(29) Bain, C. D.; Evall, J.; Whitesides, G. M. Formation of Monolayers by the Coadsorption of Thiols on Gold - Variation in the Head Group, Tail Group, and Solvent. *J. Am. Chem. Soc.* **1989**, *111*, 7155−7164.
(30) Damos, F. S.; Luz, R. C. S.; Kubota, L. T. Determination of Thickness, Dielectric Constant of Thiol Films, And Kinetics of Adsorption Using Surface Plasmon Resonance. *Langmuir* **2005**, *21*, 602−609.
(31) Karpovich, D. S.; Blanchard, G. J. Direct Measurement of the Adsorption-Kinetics of Alkanethiolate Self-Assembled Monolayers on a Microcrystalline Gold Surface. *Langmuir* **1994**, *10*, 3315−3322.
(32) Poirier, G. E. Characterization of Organosulfur Molecular Monolayers on Au(111) Using Scanning Tunneling Microscopy. *Chem. Rev.* **1997**, *97*, 1117−1127.
(33) De Renzi, V.; Lavagnino, L.; Corradini, V.; Biagi, R.; Canepa, M.; del Pennino, U. Very Low Energy Vibrational Modes As a Fingerprint of H-Bond Network Formation: L-Cysteine on Au(111). *J. Phys. Chem. C* **2008**, *112*, 14439−14445.
(34) Mateo-Marti, E.; Rogero, C.; Gonzalez, C.; Sobrado, J. M.; de Andres, P. L.; Martin-Gago, J. A. Interplay between Fast Diffusion and Molecular Interaction in the Formation of Self-Assembled Nanostructures of S-Cysteine on Au(111). *Langmuir* **2010**, *26*, 4113−4118.